Mineralogical Magazine, February 2018, Vol. 82(1), pp. 199–209

Bytízite, a new Cu-Sb selenide from Příbram, Czech Republic

PAVEL ŠKÁCHA[1,2,*], JIŘÍ SEJKORA[2] AND JAKUB PLÁŠIL[3]

[1] Mining muzeum Příbram, Hynka Kličky place 293, Příbram VI, 261 01, Czech Republic
[2] Department of Mineralogy and Petrology, National Museum, Cirkusová 1740, Prague 9 – Horní Počernice, 193 00, Czech Republic
[3] Institute of Physics ASCR, v.v.i., Na Slovance 1999/2, 18221 Praha 8, Czech Republic

[*Received 2 February 2017; Accepted 16 May 2017; Associate Editor: Andrew Christy*]

ABSTRACT

The new mineral bytízite was found in the dump of shaft No. 16, one of the mines in the Příbram uranium and base-metal district, central Bohemia, Czech Republic. Bytízite is associated with chaméanite, příbramite, giraudite, berzelianite, umangite, eskebornite, hakite, tetrahedrite, bukovite, crookesite and uraninite in a calcite-dominant gangue. The new mineral occurs as anhedral grains up to 40 μm, growing together in aggregates up to 300 μm across. Bytízite is steel-grey in colour and has a metallic lustre. Mohs hardness is *ca*. 2–3; the calculated density is 6.324 g cm^{-3}. In reflected light bytízite is grey with a yellowish hue, yellowish and brownish. Bireflectance and pleochroism are weak. Anisotropy is strong with grey to brownish rotation tints. Internal reflections were not observed. The empirical formula, based on electron-microprobe analyses, is $(Cu_{3.00}Fe_{0.01}Ag_{0.01})_{3.02}(Sb_{0.97}As_{0.06})_{1.03}Se_{2.94}$. The ideal formula is Cu_3SbSe_3, which requires Cu 34.71, Sb 22.16 and Se 43.13, total 100.00 wt.%. Bytízite is orthorhombic, *Pnma*, a = 7.9594(12), b = 10.5830(14), c = 6.8240(11) Å, with V = 574.82(15) Å^3 and Z = 4. The strongest reflections of the calculated powder X-ray diffraction pattern [d, Å (I)(*hkl*)] are: 3.73(37)(210), 3.27(62)(211), 2.867 (40)(022), 2.698(100)(122) and 2.646(37)(040). According to the single-crystal X-ray diffraction data (R_{obs} = 0.0437), bytízite is isostructural with synthetic Cu_3SbSe_3. The structure of bytízite contains two Cu, one Sb, and two Se sites (the latter is occupied both by Se and S atoms). In the structure of both synthetic Cu_3SbSe_3 and bytízite, there are groups of three *cis*-edge-sharing tetrahedra [Cu_3Se_8], which are interlinked to a 3D framework by $SbSe_3$ groups. Bytízite is named after its type locality, the Bytíz deposit, near the village Bytíz.

KEYWORDS: bytízite, new mineral, Sb-Se analogue of wittichenite, copper antimony selenide, selenide minerals, crystal structure, uranium deposit, Příbram, Czech Republic.

Introduction

BYTÍZITE is a new Cu-Sb selenide. It occurs in a complex selenide assemblage at the abandoned complex uranium and base-metal ore district of Příbram, Czech Republic, during an extensive research program focused on selenide mineralization of the Bohemian Massif (Sejkora *et al.*, 2011, 2012, 2014, 2016; Škácha, 2015; Škácha *et al.*, 2014, 2015, 2016, 2017; Sejkora and Škácha, 2015*a*,*b*).

Bytízite is named after its type locality, the Bytíz deposit, near the village of Bytíz. The Bytíz deposit is the most important within the Příbram uranium and base-metal district; it produced more than 52% of uranium from the whole district. The Příbram uranium and base-metal district is the largest vein-type uranium deposit in the Czech Republic (Litochleb *et al.*, 2003).

The new mineral and the name were approved by the Commission on New Minerals, Nomenclature and Classification of the International Mineralogical Association (IMA2016-044). The cotype material (two polished sections) is deposited in the Mineralogical collection of the Department of Mineralogy and Petrology of the National

*E-mail: skacha-p@muzeum-pribram.cz
https://doi.org/10.1180/minmag.2017.081.035

Museum, Prague, Czech Republic (catalogue number P1P 11/2016) and in the mineralogical collection of the Mining Museum Příbram, Příbram, Czech Republic, under the catalogue number 2/2016.

Occurrence

The Příbram ore area (central Bohemia, Czech Republic) is known for the deposits of base-metals as well as for uranium ores. It could be divided into two main ore districts: the base-metal Březové Hory ore district and the complex U and base-metal Příbram district. The latter represents the largest accumulation of vein-type hydrothermal U ores in the Czech Republic and is comparable to world-class deposits of this type. The hydrothermal U mineralization of late Variscan age is related to a 1–2 km wide and almost 25 km long zone formed by a strongly tectonized series of Upper Proterozoic rocks along the contact with granitoids of the Permo-carboniferous Central Bohemian Plutonic Complex. The Příbram uranium and base-metal district can be sub-divided into several ore deposits (also called ore nodes) – among them the most important were Bytíz, Háje and Brod (Ettler *et al*., 2010).

In this ore district, there are four main mineralization stages: (1) siderite–sulfides; (2) calcite; (3) calcite–uraninite; and (4) calcite–sulfides. Selenide mineralization occurs in close association with uraninite of the calcite–uraninite mineralization, but selenides are always younger than uraninite. It is uncertain whether the selenides at Příbram formed at the end of the calcite–uraninite stage, or at the beginning of the following calcite–sulfides stage. The age of the uranium mineralization obtained by U–Pb radiometric age determination of two uraninite samples is middle Permian, 275 ± 4 and 278 ± 4 Ma (Anderson, 1987).

The first selenide found there – clausthalite – was mentioned by Růžička (1986); subsequently, eight selenides were found during a study of the National museum (Prague) specimen by Litochleb *et al.* (2004). Since 2005, the first author (PŠ) has found many specimens of a selenide-containing gangue in the dump material of shafts #16, #11A and #9. The collected material contains a very rich selenide assemblage (Škácha, 2015; Škácha and Sejkora, 2007, Škácha *et al.*, 2009; 2010, 2014, 2015, 2016), including a new mineral, here described as bytízite.

One hand-sized sample with bytízite was found in mine dump material of shaft #16 (49°40′33.7″N, 14°03′30.5″E), located in the Háje deposit. Shaft #16 exploited mainly the middle and deeper parts of the vein system of the deposits Háje, Bytíz and Jerusalem (from 500 m down to a depth of 1800 m below the surface). The majority of the selenide-bearing material probably came from the ore deposit Bytíz, which provided 52% of the net U production of the entire district. The Se–U mineralization is of low-temperature hydrothermal origin and is confined to calcite veins with a thickness varying from tens of centimetres to several metres. The main ore is represented by uraninite, while younger pyrobitumen predominates in deeper parts of the deposit.

Macroscopically, bytízite forms a substantial part of up to 1 mm large steel-grey grains in a calcite vein several millimetres thick. This younger carbonate vein cuts perpendicularly through an older calcite vein containing common umangite and uraninite, so umangite is unequivocally older than other selenides in the association. Bytízite forms anhedral grains enclosing other coexisting selenides which involves chaméanite $(Cu,Fe)_4As(Se,S)_4$, bukovite $Tl_2(Cu,Fe)_4Se_4$, příbramite $CuSbSe_2$, eskebornite, crookesite and giraudite $(Cu_6[Cu_4(Fe,Zn)_2]As_4Se_{13}$. Therefore, bytízite appears to be the youngest selenide in the association. Hakite and tetrahedrite also occur, probably as relatively late phases in the association.

Physical and optical properties

Bytízite forms anhedral grains 10–40 μm in diameter (Fig. 1, 2), growing together in aggregates up to 300 μm across. The mineral is steel grey in colour and is opaque in transmitted light; it has a metallic lustre. No cleavage and fracture were observed. The calculated density ($Z = 4$) for the empirical formula is 6.324 g cm^{-3}. Mohs hardness is assumed at 2–3 by analogy with wittichenite and skinnerite. In reflected light, bytízite is grey with a yellowish hue and weak bireflectance. Pleochroism is weak. Anisotropy under crossed polarisers is strong (Fig. 1), with grey to brownish rotation tints. Internal reflections were not observed. Reflectance percentages for the four Commision on Ore Mineralogy wavelengths (R_{min} and R_{max}) for bytízite from Příbram are: 36.1/40.2 (470 nm), 36.1/39.3 (546 nm), 35.5/38.3 (589 nm) and 34.7/37.0 (650 nm); the full reflectance dataset are given in Table 1 and Fig. 3.

https://doi.org/10.1180/minmag.2017.081.035 Published online by Cambridge University Press

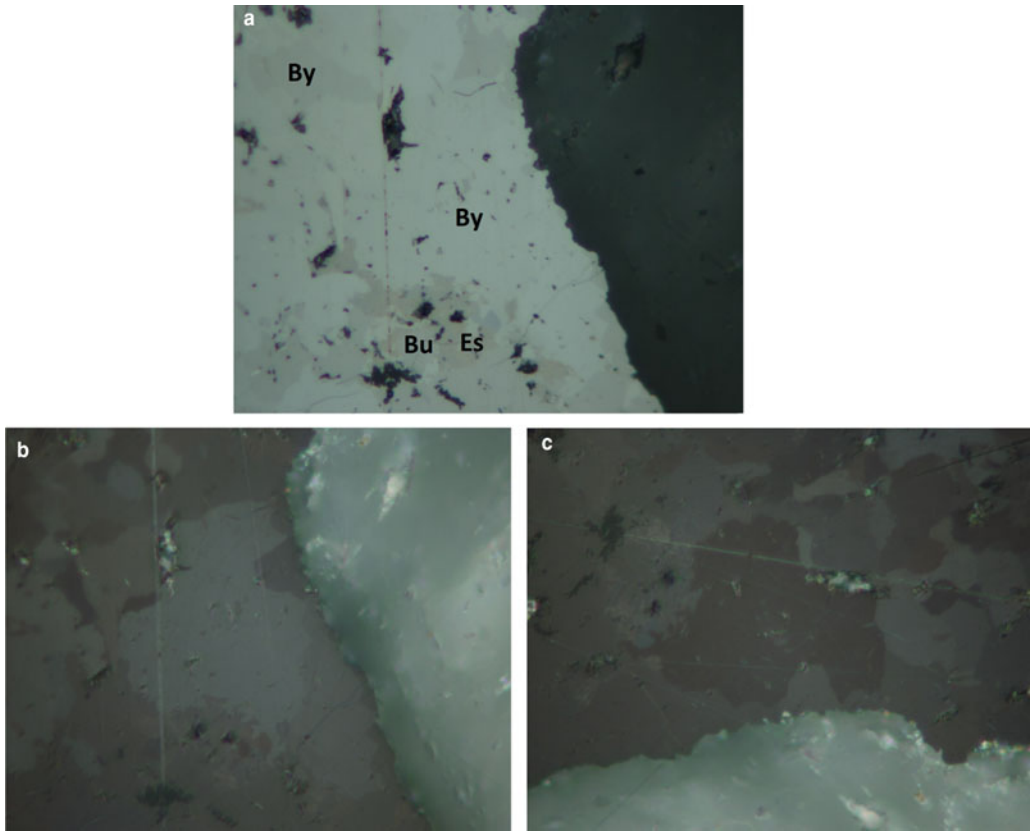

FIG. 1. Reflected light image of an aggregate (Field of view ≈ 100 μm) of bytízite (By), bukovite (Bu) and eskebornite (Es) with one nicol; (*b* and *c*) reflected light image, partly crossed polarisers (different extinction); with crossed polars, bytízite is strong anisotropic with grey to brownish rotation tints; photos: P. Škácha and J. Sejkora.

Chemical composition

Chemical analyses ($n = 68$) were performed using a Cameca SX100 electron microprobe (National Museum, Prague) operating in wavelength-dispersive mode (25 kV, 20 nA and 2 μm wide beam). Analytical data are given in Table 2 and representative analyses are given in Table 3. The following standards and X-ray lines were used to minimize line overlaps: Ag (Ag*L*α), Au (Au*M*α), Bi (Bi*M*β), CdTe (Cd*L*α), Co (Co*K*α), chalcopyrite (Cu*K*α), FeS_2 (Fe*K*α, S*K*α), HgTe (Hg*M*α), NiAs (Ni*K*α, As*L*α), PbS (Pb*M*α), PbSe (Se*L*α), PbTe (Te*L*α), Sb_2S_3 (Sb*L*α), Tl(BrI) (Tl*L*α) and ZnS (Zn*K*α). Peak counting times were 20 s for all elements, and one half of the peak time for each background. Other elements, such as Au, Bi, Cd, Co, Ni, Pb, Te, Tl and Zn were found to be below the detection limits (0.02–0.05 wt.%). Raw intensities were converted to the concentrations of elements using the automatic 'PAP' (Pouchou and Pichoir, 1985) matrix-correction software.

The chemical compositions of individual grains of bytízite are very similar, and correspond very well with the formula Cu_3SbSe_3 derived from the crystal structure study. Only minor Sb–As and S–Se substitutions were observed; a similar trend was found for other Cu-Sb selenides from Příbram, i.e. permingeatite (Škácha *et al.*, 2014) and příbramite (Škácha *et al.*, 2017). The empirical formula for bytízite, based on electron-microprobe analyses, is $(Cu_{3.00}Fe_{0.01}Ag_{0.01})_{3.02}(Sb_{0.97}As_{0.06})_{1.03}Se_{2.94}$. The ideal formula is Cu_3SbSe_3, which requires Cu 34.71, Sb 22.16 and Se 43.13, total 100.00 wt.%.

X-ray diffraction data

The powder X-ray study was carried out using a Rigaku (Oxford Diffraction) SuperNova single-crystal diffractometer with Atlas S2 CCD detector

https://doi.org/10.1180/minmag.2017.081.035 Published online by Cambridge University Press

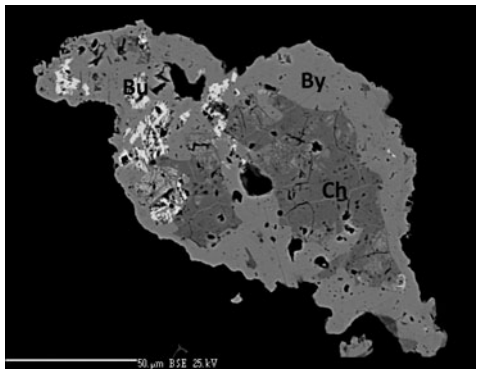

FIG. 2. Back-scatter electron image of a bytízite aggregate (By) enclosed anhedral grains of bukovite (Bu) and chaméanite (Ch). Photo: J. Sejkora and P. Škácha.

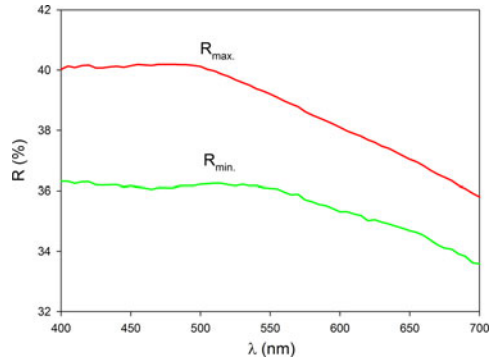

FIG. 3. Reflectivity curves for bytízite.

utilizing Mo*K*α radiation provided by the micro-focus X-ray tube and monochromatized by primary mirror optics. A Gandolfi-like motion on the ϕ and ω axes was used to randomize the sample and observed *d* spacings and intensities were derived using *CrysAlis* software (Rigaku, 2016). The powder data presented in Table 4 show good agreement with the pattern calculated from the structure determination. Unit-cell parameters refined from the powder data using *Celref* (Laugier and Bochu, 2003) are: $a = 7.94(1)$, $b = 10.55(3)$, $c = 6.84(1)$ Å and $V = 573(1)$ Å^3.

A 0.02 mm × 0.01 mm × 0.01 mm large crystal of bytízite, extracted from the polished section, was examined using a Rigaku (Oxford Diffraction) SuperNova single-crystal diffractometer with Atlas S2 CCD detector utilizing Mo*K*α radiation provided by the micro-focus X-ray tube and monochromatized by primary mirror optics. The ω rotational scans (frame width of 1.0° and counting time of 250 s) were adopted for the acquisition of the three dimensional intensity data. From the total of 8231 reflections, 809 were independent and 590 classified as unique observed with $I > 3\sigma(I)$. Corrections for background, Lorentz effects and polarization were applied during data-reduction in the *CrysAlis* software, a correction for absorption, using Gaussian integration ($\mu = 34.44$ mm^{-1}) were applied in *Jana2006* (Petříček *et al.*, 2014) to the data, with R_{int} of 0.117. The structure of bytízite was refined from diffraction data based on the structure model for synthetic orthorhombic Cu_3SbSe_3 (Pfitzner, 1995) by the full-matrix least-squares algorithm of the *Jana2006* program. All atoms were refined with anisotropic atomic displacement parameters. Refinement for 37 parameters converged smoothly to the final $R = 0.0437$,

TABLE 1. Reflectance values (WTiC standard in air, Zeiss 370; spectrophotometer MSP400 TIDAS with Leica microscope, objective 50x). Data are plotted in Fig. 1.

$R_{min.}/R_{max.}$	λ (nm)	$R_{min.}/R_{max.}$	λ (nm)
36.3/40.0	400	36.0/39.0	560
36.3/40.2	420	35.6/38.5	580
36.2/40.1	440	**35.5/38.3**	**589**
36.1/40.2	460	35.3/38.1	600
36.1/40.2	**470**	35.0/37.7	620
36.1/40.2	480	34.8/37.3	640
36.2/40.1	500	**34.7/37.0**	**650**
36.2/39.8	520	34.5/36.8	660
36.2/39.4	540	34.1/36.3	680
36.1/39.3	**546**	33.6/35.8	700

Note: The values required by the Commission on Ore Mineralogy are given in bold.

TABLE 2. Compositional data (wt.%) for bytízite ($n = 68$).

Constituent	Mean	Range	SD	Probe standard
Ag	0.25	0.08–1.54	0.26	Ag
Cu	34.64	31.98–36.23	0.85	$CuFeS_2$
Fe	0.07	0.00–0.37	0.10	FeS_2
Hg	0.04	0.00–0.75	0.16	HgTe
Sb	21.39	19.07–22.51	0.74	Sb_2S_3
As	0.80	0.18–2.09	0.47	NiAs
Se	42.19	40.65–43.33	0.58	PbSe
S	0.08	0.00–0.93	0.15	FeS_2
Total	99.46			

SD – Standard deviation

https://doi.org/10.1180/minmag.2017.081.035 Published online by Cambridge University Press

TABLE 3. Representative analyses (wt.%) for bytízite*.

	Ideal	Mean	1	2	3	4	5	6	7	8	9	10	11	12	13	14	15
Ag	0.00	0.25	0.14	0.09	0.10	0.22	0.59	0.12	0.15	0.75	0.22	0.16	0.12	0.79	0.43	1.54	0.13
Fe	0.00	0.07	0.10	0.11	0.00	0.30	0.20	0.00	0.06	0.00	0.03	0.00	0.00	0.50	0.51	0.30	0.00
Hg	0.00	0.04	0.00	0.05	0.00	0.07	0.00	0.00	0.00	0.15	0.00	0.00	0.00	1.35	0.00	0.75	0.08
Cu	34.71	34.64	34.30	34.12	34.38	33.79	33.21	34.92	35.13	35.13	34.60	34.52	35.09	31.80	33.48	33.46	36.23
Sb	22.16	21.39	21.82	21.13	21.37	21.33	20.79	21.37	21.27	21.27	22.66	22.10	20.95	19.51	21.23	19.07	19.98
As	0.00	0.80	0.71	0.83	0.69	0.81	0.92	0.94	1.01	0.48	0.00	0.46	1.33	1.68	0.34	1.95	2.09
Se	43.13	42.19	42.25	42.39	41.86	41.74	44.03	41.82	41.72	42.64	41.89	41.50	42.34	43.33	43.92	42.79	40.65
S	0.00	0.00	0.00	0.00	0.00	0.00	0.00	0.00	0.00	0.00	0.00	0.00	0.00	0.00	0.00	0.00	0.93
Total	100.00	99.46	99.36	98.78	98.48	98.36	99.74	99.22	99.40	100.47	99.45	98.79	99.89	99.23	99.98	99.94	100.08
Ag	0.000	0.013	0.007	0.005	0.005	0.011	0.030	0.006	0.008	0.038	0.011	0.008	0.006	0.041	0.022	0.078	0.007
Fe	0.000	0.007	0.009	0.011	0.000	0.030	0.020	0.000	0.006	0.000	0.003	0.000	0.000	0.050	0.050	0.029	0.000
Cu	3.000	3.000	2.980	2.975	3.008	2.961	2.875	3.029	3.038	3.016	3.012	3.018	3.016	2.785	2.887	2.886	3.053
Σ*M*	3.000	3.019	2.996	2.990	3.013	3.002	2.925	3.035	3.051	3.054	3.027	3.026	3.022	2.875	2.959	2.994	3.059
Sb	1.000	0.967	0.989	0.962	0.976	0.976	0.939	0.968	0.960	0.953	1.030	1.008	0.940	0.892	0.956	0.859	0.878
As	0.000	0.059	0.052	0.061	0.051	0.060	0.068	0.069	0.074	0.035	0.000	0.034	0.097	0.125	0.025	0.143	0.149
ΣSb + As	1.000	1.026	1.041	1.023	1.027	1.036	1.007	1.037	1.034	0.988	1.030	1.043	1.037	1.016	0.980	1.001	1.028
Se	3.000	2.940	2.954	2.974	2.947	2.943	3.068	2.919	2.903	2.946	2.935	2.920	2.930	3.053	3.048	2.971	2.756
S	0.000	0.000	0.000	0.000	0.000	0.000	0.000	0.000	0.000	0.000	0.000	0.000	0.000	0.000	0.000	0.000	0.155
ΣSe + S	3.000	2.940	2.954	2.974	2.947	2.943	3.068	2.919	2.903	2.946	2.935	2.920	2.930	3.053	3.048	2.971	2.911

*1–15 representative analyses of bytízite from Příbram; coefficients of the empirical formula were calculated on the basis of 7 atoms per formula unit.

TABLE 4. Powder X-ray diffraction data (*d* in Å) for bytízite*.

I_{obs}	d_{obs}	d_{calc}	I_{calc}	*h*	*k*	*l*	I_{obs}	d_{obs}	d_{calc}	I_{calc}	*h*	*k*	*l*
		3.98	12	2	0	0			1.869	21	2	5	0
30	3.74	3.73	37	2	1	0	30	1.86	1.863	30	4	2	0
		3.70	12	1	2	1			1.859	20	1	3	3
10	3.43	3.41	15	0	0	2			1.850	13	2	2	3
50	3.27	3.27	62	2	1	1			1.802	22	2	5	1
		3.18	10	2	2	0	25	1.79	1.801	32	3	3	2
25	3.01	3.01	19	1	1	2			1.797	13	4	2	1
		2.916	22	1	3	1			1.764	16	0	6	0
35	2.88	2.867	40	0	2	2			1.754	8	1	5	2
		2.698	100	1	2	2	10	1.72	1.727	9	3	0	3
100	2.68	2.646	37	0	4	0			1.723	7	2	3	3
		2.640	22	2	3	0	10	1.67	1.668	7	1	0	4
10	2.59	2.590	6	2	0	2			1.642	8	3	4	2
20	2.48	2.473	23	3	0	1	10	1.63	1.639	6	2	5	2
		2.408	5	3	1	1			1.624	8	0	2	4
		2.097	6	2	4	1			1.590	5	4	4	0
20	2.09	2.095	12	3	0	2	10	1.53	1.534	6	5	1	1
		2.091	19	2	3	2	10	1.43	1.443	6	5	0	2
10	2.03	2.022	19	1	4	2			1.436	6	3	6	1
		1.948	10	3	2	2			1.226	5	0	6	4
15	1.94	1.941	6	2	1	3	15	1.22	1.222	12	6	3	1
		1.910	9	4	0	1			1.219	8	1	8	2

*The calculated diffraction pattern was obtained with the atom coordinates reported in Table 6 (only reflections with $I_{rel.} \geq 4$ are listed).

wR = 0.0898 for 530 observed reflections with Goof = 1.30. Details of data collection, crystallographic data and refinement are given in Table 5. Atom coordinates and displacement parameters are listed in Table 6; selected interatomic distances and bond-valence sums are provided in Table 7. The bond-valence parameters were taken from Shields *et al.* (2000) for Cu^{1+}–Se and from Brown (pers. comm.) for Sb^{3+}–Se.

On the basis of the current X-ray study we conclude bytízite is orthorhombic, which is in line with the studies on synthetic Cu_3SbSe_3 prepared by Pfitzner (1995). The structure of bytízite (Fig. 4) contains two Cu sites, one Sb site and two Se sites, all sites were assumed to be fully occupied. The Cu1 site is 3 + 1 coordinated by three Se atoms at a distance of ~2.4 Å and one longer Cu–Se bond, ~2.88 Å (Table 7; Fig. 5). The Cu2 site is regularly coordinated by four Se atoms to form a tetrahedron. The Sb site is coordinated by three Se atoms as a regular trigonal pyramid (Fig. 5). There is no departure from the structure of synthetic orthorhombic Cu_3SbSe_3 (Pfitzner, 1995). In the structure of both synthetic Cu_3SbSe_3 and bytízite there are groups of three *cis*-edge-sharing tetrahedra [Cu_3Se_8], which are interlinked to a 3D framework by $SbSe_3$ groups (Fig. 4). Wittichenite, Cu_3BiS_3 (Kocman and Nuffield, 1973) possesses a similar structure to bytízite, synthetic Cu_3SbSe_3 phases (Pfitzner, 1995) and skinnerite (Karup-Møller and Makovicky, 1974; Makovicky and Balič-Žunič, 1995); however, there are substantial differences among these structures. While in the case of bytízite, synthetic Cu_3SbSe_3 and skinnerite, one of the Cu sites is tetrahedrally coordinated, in wittichenite all Cu atoms are in a three-fold planar coordination. As reported by Makovicky and Balič-Žunič (1995), in wittichenite, the Cu atoms are *cis*-oriented around octahedral voids, while in the rest of the above mentioned phases, two distinct types of configuration occur: *cis*- and *trans*- patterns alternate in layers, as a consequence of the smaller size of SbS_3 (as well as $SbSe_3$) compared to BiS_3 pyramids.

Relationship to the known species

As mentioned previously, bytízite (Strunz class 2/E.03-40, Dana class 3.4.8.4) is related structurally

https://doi.org/10.1180/minmag.2017.081.035 Published online by Cambridge University Press

TABLE 5. Summary of data collection conditions and refinement parameters for bytízite.

Structural formula	Cu_3SbSe_3
Unit-cell parameters	
a [Å]	7.9594(12)
b [Å]	10.5830(14)
c [Å]	6.8240(11)
V [Å^3]	574.82(15)
Z	4
Space group	*Pnma*
D_{calc} (g.cm^{-3})	6.347
Temperature	296 K
Wavelength	Mo*K*α (0.71073 Å)
Crystal dimensions (mm)	0.022 × 0.010 × 0.009
Collection mode	ω scans to fill Ewald sphere
Limiting θ angles	3.55–29.68°
Limiting Miller indices	$-11 \le h \le 10$ $-14 \le k \le 14$ $-9 \le l \le 8$
No. of reflections	8231
No. of unique reflections	809
No. of observed reflections (criterion)	590 [$I > 3\sigma(I)$]
Absorption correction (mm^{-1}), method	34.44, Gaussian
T_{min}/T_{max}	0.650/0.876
R_{int}	0.117
F_{000}	960
Parameters/ constraints/ restraints	37/0/0
R, *wR* (obs)	0.0437, 0.0898
R, *wR* (all)	0.0781, 0.1041
Goof (obs, all)	1.30, 1.28
Weighting scheme, weights	σ. $1/(\sigma^2(F) + 0.0010863617F^2)$
$\Delta_{\rho min}$, $\Delta_{\rho max}$ (e^- Å^{-3})	−2.38, 2.96

to the high temperature (>121°C) orthorhombic modification of natural monoclinic skinnerite Cu_3SbS_3 (Karup-Møller and Makovicky, 1974; Pfitzner, 1994; Makovicky and Balič-Žunič, 1995). The synthetic analogue of bytízite has been prepared by Pfitzner (1995) in a sealed tube containing Cu, Sb and Se at 350°C for 3 weeks. Comparative data for bytízite and relevant natural and synthetic phases are given in Table 8.

Origin of the selenium mineralization in Příbram

Several selenide assemblages have been found in Příbram, where 24 selenides have been identified so far (Škácha *et al.*, 2017). One of the main reasons

TABLE 6. Atom positions and displacement parameters (Å^2) for bytízite.

Atom	*x/a*	*y/b*	*z/c*	U_{eq}	U^{11}	U^{22}	U^{33}	U^{12}	U^{13}	U^{23}
Sb	0.24997(13)	¼	0.88883(14)	0.0168(3)	0.0159(5)	0.0177(6)	0.0169(5)	0	−0.0022(4)	0
Se1	0.00571(19)	¼	0.1352(2)	0.0156(5)	0.0194(8)	0.0130(8)	0.0145(7)	0	−0.0004(6)	0
Cu1	0.0916(2)	0.04217(16)	0.2430(2)	0.0326(5)	0.0239(8)	0.0211(8)	0.0529(11)	0.0049(7)	0.0092(7)	0.0064(8)
Cu2	0.1906(3)	¼	0.4298(3)	0.0339(8)	0.0488(15)	0.0299(13)	0.0229(11)	0	−0.0070(10)	0
Se2	0.16059(13)	0.06614(10)	0.65605(14)	0.0147(3)	0.0165(6)	0.0146(6)	0.0132(5)	−0.0003(5)	−0.0009(4)	0.0019(4)

https://doi.org/10.1180/minmag.2017.081.035 Published online by Cambridge University Press

for the species diversity of the studied Se mineralization is the crystallization of a part of selenides from late hydrothermal solutions containing remobilized Sb, As, Cu, Hg, Ag and Fe.

According to observation of >120 polished sections, crystallization of first selenides started after formation of colloform uraninite (pitchblende), with Pb and Hg selenides (clausthalite, tiemannite) and eucairite, followed by a Cu–Se mineralization represented by berzelianite, umangite, klockmannite, athabascaite and bellidoite. Minerals of the tetrahedrite group (hakite and giraudite) are younger than Cu selenides in most cases. Bytízite is the result of the youngest mobilization processes together with antimonselite, hakite, příbramite, chaméanite and other selenides. The temperature of this hydrothermal solution was ~100°C, according to the presence of umangite in the association (Simon and Essene, 1996). It is in accordance with the homogenization temperatures of the fluid inclusions determined in the Příbram uranium district (Žák and Dobeš, 1991).

The abundance of calcite in gangue indicates a neutral to weakly alkaline environment (Dymkov, 1985; Kvaček, 1987). Selenides are formed from hydrothermal fluids at conditions of f_{O_2} above the hematite-magnetite buffer, probably in the range of 5.8 log units (hematite-ferroselite univariant reaction) to 7 log units (anglesite-galena buffer), above the hematite-magnetite buffer (Simon *et al.*, 1997). Such high oxygen fugacity values result in geochemical separation of selenium from sulfur in the hydrothermal fluids, a high Se_2/S_2 fugacity ratio, and in the deposition of various selenide minerals. The quantity and variability of selenide association, which formed under oxidizing

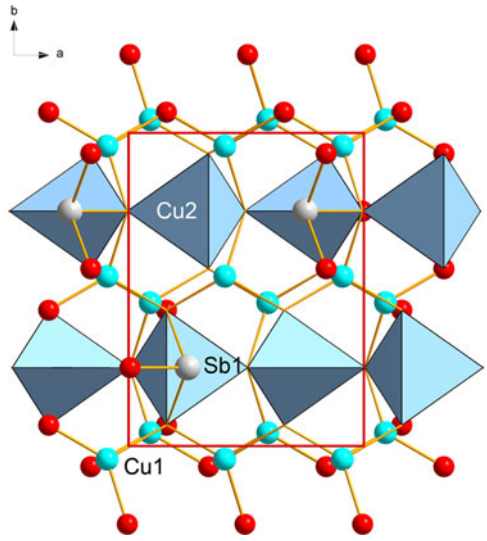

FIG. 4. Crystal structure of bytízite: Cu1 atoms (blue trigonal base) occur in 3 + 1 coordination, the Cu2 atom is coordinated as regular tetrahedron and the Sb1 atom (grey) is in trigonal pyramidal coordination. Unit-cell edges are outlined in red solid lines, the viewing direction is along [001].

TABLE 7. Interatomic distances (in Å) in the structure of bytízite and bond-valence sums (in valence units).

Sb–Se1	2.5703(18)
Sb–Se2^{i}	2.6107(17)
Sb–Se2^{ii}	2.6107(17)
Cu1–Se1	2.418(2)
Cu1–Se1^{iii}	2.418(2)
Cu1–Cu2	2.662(2)
Cu1–Se2	2.357(3)
Cu1–Se2^{i}	2.883(3)
Cu1–Se2^{v}	2.412(3)
Cu2–Se1	2.492(3)
Cu2–Se1^{iv}	2.547(4)
Cu2–Se2^{i}	2.495(2)
Cu2–Se2^{ii}	2.495(2)
Bond-valence sums	
Sb	3.027(7)
Se1	1.953(6)
Se2	1.783(4)
Cu1	0.858(2)
Cu2	0.776(2)

Symmetry codes: (i) $-x+3/2, -y+1, z-1/2$; (ii) $-x+3/2, y-1/2, z-1/2$; (iii) $x, -y+1/2, z$; (iv) $x-1/2, -y+1/2, -z+3/2$; (v) $x+1/2, y, -z+3/2$.

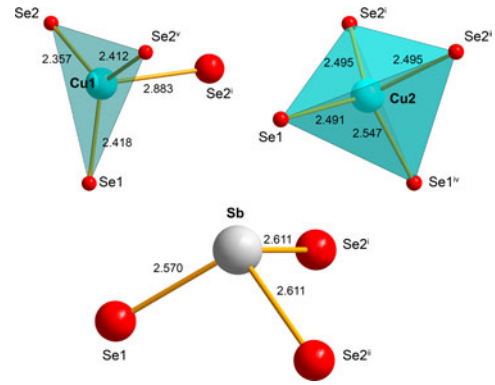

FIG. 5. Coordinations of cations found in the bytízite crystal structure. The symbols of symmetry operations are related to those in Table 7.

https://doi.org/10.1180/minmag.2017.081.035 Published online by Cambridge University Press

TABLE 8. Comparative data for the relevant minerals.

Locality	Bytízite Příbram (CZ)	Bytízite synthetic	Wittichenite Wittichen (Germany)	Skinnerite Ilímaussaq (Greenland)	High temperature modification of skinnerite – synt.
Reference	this proposal	Pfitzner (1995)	Kocman and Nuffield (1973)	Karup-Møller and Makovicky (1974)	Pfitzner (1994)
Ideal composition	Cu_3SbSe_3	Cu_3SbSe_3	Cu_3BiS_3	Cu_3SbS_3	Cu_3SbS_3
Empirical composition	$(Cu_{3.00}Ag_{0.01}Fe_{0.01})_{3.02}(Sb_{0.97}As_{0.06})_{1.03}Se_{2.94}$	Cu_3SbSe_3	$Cu_{2.98}Bi_{1.02}S_{2.99}$	$(Cu_{3.00}Ag_{0.08})_{3.08}Sb_{0.99}S_{2.94}$	Cu_3SbS_3
Space group	*Pnma*	*Pnma*	$P2_12_12_1$	$P2_1/c$	*Pnma*
a	7.9594(12)	7.9865(8)	7.723(10)	7.815(1)	7.828(3)
b	10.5830(14)	10.6138(9)	10.395(10)	10.252(3)	10.276(4)
c	6.8240(11)	6.8372(7)	6.716(5)	13.270(2)	6.604(3)
β	90°	90°	90°	90°21′(1)	90°
V	574.82(15)	579.6(1)	539.16	1063.16	531.2(2)
Z	4	4	4	8	4
Strongest lines of the powder XRD pattern	3.73/37 3.27/62 2.867/40 2.698/100 2.646/37	3.7375/36* 3.2795/68 2.8739/37 2.7042/100 2.6535/36	4.555/34* 3.186/43 3.080/81 2.860/100 2.649/47	3.910/60 3.111/60 3.048/70 2.831/100 2.628/40	

* Calculated from the structure data.

conditions, is a function of Se_2 fugacity and reflects the concentration of available Se in solutions (Simon *et al.*, 1997). The selenide mineralization in the Příbram uranium district shows variations in Se_2 and S_2 fugacities (–12 to –18 in the case of Se and –17 to –24 of S, respectively), which are similar to those published in detail (Simon *et al.*, 1997) for "selenide-bearing unconformity-related uranium deposits". Considering the absence of kruťaite from the association despite its stability at 100°C and sufficiently high f_{Se_2} (Simon *et al.*, 1997), we believe the Se mineralization to have occurred at Se fugacities too low for kruťaite stability, $\log f_{Se_2} <$ –12 (Škácha *et al.*, 2017).

Acknowledgements

The authors appreciate the comments of two anonymous reviewers, Pete Leverett and the Principal Editor Peter Williams. The research was financially supported by the project GA14-27006S of the Czech Science Foundation for PŠ a JS. Single-crystal X-ray diffraction experiments were done using instruments of the ASTRA lab established within the Operation program Prague Competitiveness – project CZ.2.16/3.1.00/24510.

References

Anderson, E.B. (1987) *Isotopic-geochronological investigation of the uranium mineralization of Czechoslovakia*. Unpublished Czechoslovak Uranium Industry Report 1962–87.

Dymkov, J. (1985) Selenidy nasturan-karbonatnych žil. Pp. 153–162 in: *Paragenezis mineralov uranonosnych žil*. Nedra, Moscow.

Ettler, V., Sejkora, J., Drahota, P., Litochleb, J., Pauliš, P., Zeman, J., Novák, M. and Pašava, J. (2010) Příbram and Kutná Hora mining districts – from historical mining to recent environmental impact. Pp. 1–23 in: *Acta Mineralogica-petrographica, Field Guide Series* 7. IMA 2010, Budapest.

Karup-Møller, S. and Makovicky, E. (1974) Skinnerite, a new sulfosalt from the Ilimaussaq Alkaline Intrusion, South Greenland. *American Mineralogist*, **59**, 889–895.

Kocman, V. and Nuffield, E.W. (1973) The crystal structure of wittichenite, Cu_3BiS_3. *Acta Crystalographica*, **B29**, 2528–2535.

Kvaček, M. (1987) Mineralogicko – geochemická charakteristika selenidového zrudnění na uranových ložiskách Českého masivu. In: *Mineralogia uránových a s nimi súvisiacích nerastných surovín*. Sborník Spišská Nová Ves, 89–95.

Laugier, J. and Bochu, B. (2003) *CELREF: Unit Cell Refinement Program from Powder Diffraction Diagram*. Laboratoires des Matériaux et du Génie Physique, Ecole Nationale Supériaux de Physique de Grenoble (INPG), Grenoble, France.

Litochleb, J., Černý, P., Litochlebová, E., Sejkora, J. and Šreinová, B. (2003) The deposits and occurrences of mineral raw materials in the Střední Brdy Mts. and the Brdy piedmont area (Central Bohemia). *Bulletin mineralogicko – petrologického oddělení Národního muzea v Praze*, **11**, 57–86.

Litochleb, J., Sejkora, J. and Šrein, V. (2004) Selenides from the Bytíz deposit (Příbram uranium and base-metal district). *Bulletin mineralogicko – petrologického oddělení Národního muzea v Praze*, **12**, 113–123.

Makovicky, E. and Balič-Žunič, T. (1995) The crystal structure of skinnerite, $P2_1/c$-Cu_3SbS_3, from powder data. *The Canadian Mineralogist*, **33**, 655–663.

Petříček, V., Dušek, M. and Palatinus, L. (2014) Crystallographic computing system Jana 2006: general features. *Zeitschrift für Kristallographie*, **229**, 345–352.

Pfitzner, A. (1994) Cu_3SbS_3: Zur Kristallstruktur und Polymorphie. *Zeitschrift für anorganische und allgemeine Chemie*, **620**, 1992–1997.

Pfitzner, A. (1995) Cu_3SbSe_3, Synthese und Kristallstruktur. *Zeitschrift für anorganische und allgemeine Chemie*, **621**, 685–688.

Pouchou, J.L. and Pichoir, F. (1985) "PAP" (πρZ) procedure for improved quantitative microanalysis. Pp. 104–106 in: *Microbeam Analysis* (J.T. Armstrong, editor). San Francisco Press, San Francisco, California, USA.

Rigaku (2016) *CrysAlis CCD and CrysAlis RED*. Oxford Diffraction Ltd, Yarnton, Oxfordshire, UK.

Růžička, J. (1986) Minerals of the Příbram uranium deposit. *Komitét symposia Hornická Příbram ve vědě a technice*, Příbram, 1–244.

Sejkora, J. and Škácha, P. (2015*a*) Selenides from the fluorite deposit Moldava, Krušné hory Mountains (Czech Republic). *Bulletin mineralogicko – petrologického oddělení Národního muzea v Praze*, **23**, 229–241.

Sejkora, J. and Škácha, P. (2015*b*) The occurence of selenides at the deposit Běstvina, Železné hory Mountains (Czech Republic). *Bulletin mineralogicko – petrologického oddělení Národního muzea v Praze*, **23**, 255–260.

Sejkora, J., Makovicky, E., Topa, D., Putz, H., Zagler, G. and Plášil, J. (2011) Litochlebite, $Ag_2PbBi_4Se_8$, a new selenide mineral species from Zálesí, Czech Republic: description and crystal-structure. *The Canadian Mineralogist*, **49**, 639–650.

Sejkora, J., Plášil, J., Litochleb, J., Škácha, P. and Pavlíček, R. (2012) A selenide association with macroscopic umangite from the abandoned uranium deposit Zálesí, Rychlebské hory Mountains (Czech Republic). *Bulletin mineralogicko – petrologického oddělení Národního muzea v Praze*, **20**, 187–196.

https://doi.org/10.1180/minmag.2017.081.035 Published online by Cambridge University Press

Sejkora, J., Macek, I., Škácha, P., Pauliš, P., Plášil, J. and Toegel, V. (2014) An occurrence of Hg and Tl selenides at the abandoned uranium deposit Zálesí, Rychlebské hory Mountains (Czech Republic). *Bulletin mineralogicko – petrologického oddělení Národního muzea v Praze*, **22**, 333–345.

Sejkora, J., Škácha, P., Kopecký, S. sen., Kopecký, S. jun., Pauliš, P., Malíková, R. and Velebil, D. (2016) Se and Cu mineralization from Bílá Voda near Javorník (Czech Republic). *Bulletin mineralogicko – petrologického oddělení Národního muzea v Praze*, **24**, 2, 161–177.

Shields, G.P., Raithby, P.R., Allen, F.H. and Motherwell, W. D.S. (2000) The assignment and validation of metal oxidation states in the Cambridge Structural Database. *Acta Crystalographica*, **B56**, 455–465.

Simon, G. and Essene, E.J. (1996) Phase relations among selenides, sulphides, tellurides, and oxides: I. Thermodynamic properties and calculated equilibria. *Economic Geology*, **91**, 1183–1208.

Simon, G., Kesler, S.E. and Essene, E.J. (1997) Phase relations among selenides, sulphides, tellurides, and oxides: II. Applications to selenide-bearing ore deposits. *Economic Geology*, **92**, 468–484.

Škácha, P. (2015) *Role of the selenium in the late hydrothermal phase of the Příbram uranium region*. Unpublished PhD Thesis, Charles University, Prague, Czech Republic, 235 p.

Škácha, P. and Sejkora, J. (2007) Arsenolamprite occurrence in the Příbram uranium and base-metal district. *Bulletin mineralogicko – petrologického oddělení Národního muzea v Praze*, **14–15**, 131–133.

Škácha, P., Sejkora, J., Litochleb, J. and Hofman, P. (2009) Cuprostibite occurrence in the Příbram uranium and base-metal district (shaft No. 16, Příbram - Háje), Czech Republic. *Bulletin mineralogicko - petrologického oddělení Národního muzea v Praze*, **17**(1), 73–78.

Škácha, P., Vlček, V., Sejkora, J., Plášil, J. and Goliáš, V. (2010): Compositional trends in hakite, possible discrepancies from ideal structure. *Acta Mineralogica-petrographica*, Abstract Series **6**, 725.

Škácha, P., Buixaderas, E., Plášil, J., Sejkora, J., Goliáš, V. and Vlček, V. (2014) Permingeatite, Cu_3SbSe_4, from Příbram (Czech Republic): description and Raman spectroscopy investigations of the luzonite-subgroup of minerals. *The Canadian Mineralogist*, **52**, 501–511.

Škácha, P., Plášil, J., Sejkora, J. and Goliáš, V. (2015) Sulphur-rich antimonselite, $Sb_2(Se,S)_3$ in the Se-bearing mineral association from the uranium and base metal ore district Příbram, Czech Republic. *Journal of Geosciences*, **60**(1), 23–29.

Škácha, P., Palatinus, L., Sejkora, J., Plášil, J., Macek, I. and Goliáš, V. (2016) Hakite from Příbram, Czech Republic: Compositional variability, crystal structure and the role within the Se-mineralization. *Mineralogical Magazine*, **80**(6), 1–15.

Škácha, P., Sejkora, J. and Plášil, J. (2017) Příbramite, $CuSbSe_2$, the Se-analogue of chalcostibite, a new mineral from Příbram, Czech Republic. *European Journal of Mineralogy*, **29**, 653–661.

Žák, K. and Dobeš, P. (1991) Stable isotopes and fluid inclusions in hydrothermal deposits: the Příbram ore region. *Rozpravy Československé akademie věd*, Řada Matematických a Přírodních Věd, **101**, 1–109.

https://doi.org/10.1180/minmag.2017.081.035 Published online by Cambridge University Press